

---

# A Decade of Computer Simulations for Space Shuttle Aerodynamics

---

Mamoru Inouye

---

May 1988

LIBRARY

JUL 18 1988

LANGLEY RESEARCH CENTER  
RESEARCH DIVISION  
HAMPTON, VIRGINIA

**NASA**

National Aeronautics and  
Space Administration

---

# A Decade of Computer Simulations for Space Shuttle Aerodynamics

---

Mamoru Inouye, Ames Research Center, Moffett Field, California

May 1988



National Aeronautics and  
Space Administration

**Ames Research Center**  
Moffett Field, California 94035

*N88-24603 #*

# A DECADE OF COMPUTER SIMULATIONS FOR SPACE SHUTTLE AERODYNAMICS

Mamoru Inouye

Ames Research Center

## SUMMARY

Ten years ago, computer simulations of the flow field around the Space Shuttle orbiter were limited to inviscid calculations for the windward side of the forebody and viscous calculations for selected two-dimensional problems. Advances in computer hardware and numerical methods during the past 10 years have made it possible to calculate viscous flow over the complete orbiter configuration at angle of attack. The equations solved are the Reynolds-averaged, Navier-Stokes equations, simplified by either the thin-layer or parabolized approximation. An algebraic eddy viscosity model is used for turbulent flow. The free stream is assumed to be a perfect gas for wind tunnel conditions and a real gas in thermodynamic equilibrium for flight conditions. Four examples of recent computer simulations will be presented. Flow field results include oil flow patterns on the surface and Mach number contours, isobars, and cross-flow velocity vectors in the shock layer.

## INTRODUCTION

Preliminary computer simulations of the flow field around the Space Shuttle orbiter, shown in Fig. 1, were presented at the 12th International Symposium on Space Technology and Science held in Tokyo in 1977 (Ref. 1). The results were limited to inviscid calculations for the windward side of the forebody and viscous calculations for two-dimensional problems. Advances in computer hardware and numerical methods have made it possible to calculate viscous flow over the complete orbiter configuration at angle of attack.

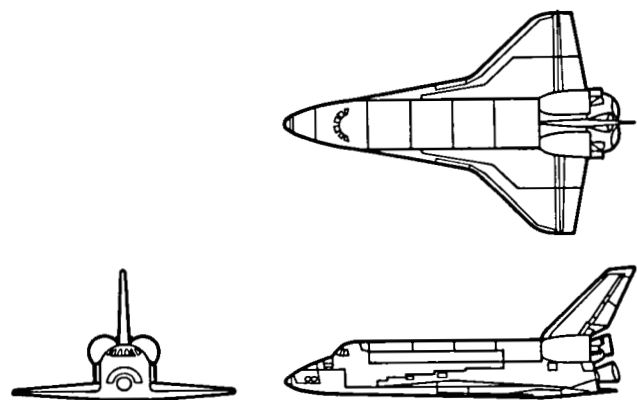


Fig. 1 Space Shuttle orbiter

Ten years ago the Control Data Corporation 7600 with a peak processing speed less than 10 million floating point

operations/sec and a main memory of half a million words was the largest computer generally available. The current generation of supercomputers was just being introduced to the scientific community, and NASA Ames Research Center had the unique ILLIAC IV. Today, supercomputers are available with peak speeds exceeding one billion floating point operations/sec and with main memories of 250 million words. Their availability extends to academia, industry, and governmental organizations worldwide as shown in Fig. 2. Advances have also been made in peripheral equipment for storing data and displaying results of computations.

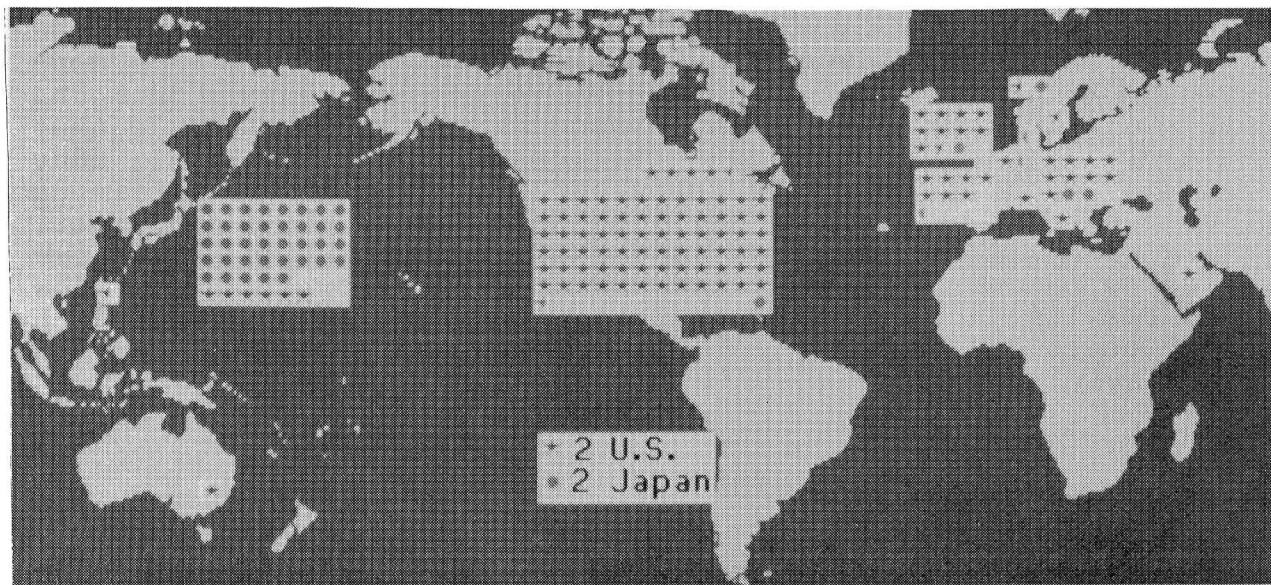


Fig. 2 Worldwide Distribution of Supercomputers

Concurrent with advances in computer speed and memory, faster numerical methods have been developed to drastically reduce the computer time required to solve complex flow fields. Ten years ago, explicit finite difference methods, which require small time steps to achieve stability, were used, and the MacCormack method was the most popular. Today, implicit methods, which are not so restricted, are used in many computer codes, and the Beam-Warming class of methods has replaced the MacCormack method in popularity. Advances in grid generation techniques also make it possible to produce physically appropriate computational meshes around complex aircraft configurations.

Four examples of recent computer simulations will be shown for viscous flow over the Space Shuttle orbiter. The equations solved are the Reynolds-averaged, Navier-Stokes equations, simplified by either the thin-layer or parabolized approximation to facilitate their solution. For the high Reynolds numbers nor-

mally associated with aerodynamic configurations, the viscous effects are confined to the neighborhood of the body, which results in the derivatives of the viscous terms normal to the surface being much larger than the corresponding derivatives along the surface. When the latter are neglected, the thin-layer approximation results. If the flow is also steady and supersonic, the parabolized Navier-Stokes equations can be obtained by simplifying the streamwise pressure gradient within the viscous layer. In this case the resulting equations may be solved by a space-marching method, proceeding downstream step by step from one cross-sectional plane to another. Available computer storage can be used effectively for this approach because just a fraction of the flow field properties need be stored at any given time. The solution algorithms used in the following examples are all based on the implicit Beam-Warming method.

## RESULTS

### Example 1

The first example is a solution by Chaussee, Rizk, and Buning (Ref. 2) for the parabolized Navier-Stokes equations with a perfect gas free stream representative of wind tunnel condi-

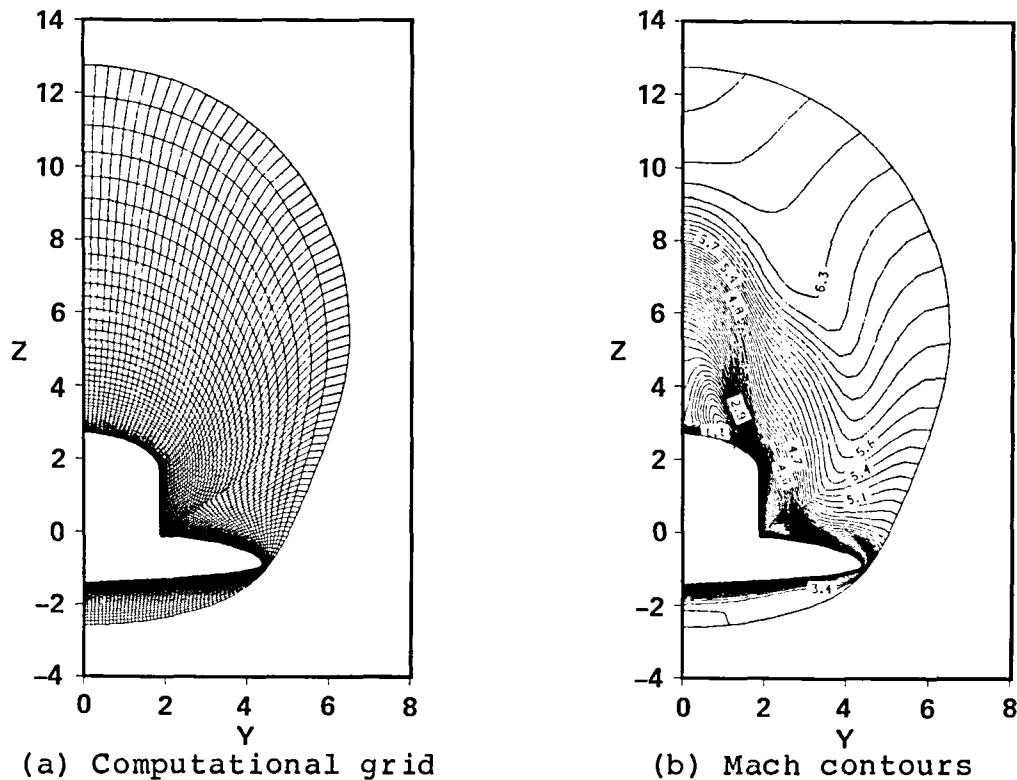


Fig. 3 Perfect gas solution,  $M_\infty = 7.9$ ,  $\alpha = 25^\circ$ ,  $x/L = 0.66$   
(Ref. 2)

tions. The free-stream Mach number,  $M_\infty$ , was 7.9, the angle of attack,  $\alpha$ , was  $25^\circ$ , and the Reynolds number based on vehicle length was 1.37 million. Turbulent flow was assumed over the surface with the eddy viscosity calculated from the Baldwin-Lomax algebraic model (Ref. 3). The calculations were initiated at the cross section located at  $x/L = 0.0522$ , where  $x$  is the axial distance measured from the nose and  $L$  is the total length of the orbiter. The axial flow was supersonic at this cross section, and flow properties were obtained from a blunt body code. The flow field properties were then marched downstream as far as the cross section,  $x/L = 0.66$ , where the interaction of the bow shock wave with the wing shock caused a local subsonic region which invalidated the solution procedure. The computational grid at  $x/L = 0.66$  is shown in Fig. 3a. The outer boundary is the bow shock wave, and points are clustered near the surface to resolve the viscous layer. Mach number contours are shown in Fig. 3b, where coalescence of contours indicates the locations of the wing shock and cross flow shocks on the wing and upper body. Simulated oil flow patterns over the upper orbiter surface are shown in Fig. 4. Separated flow is indicated on the strake-wing and payload bay door on the upper half of the fuselage.

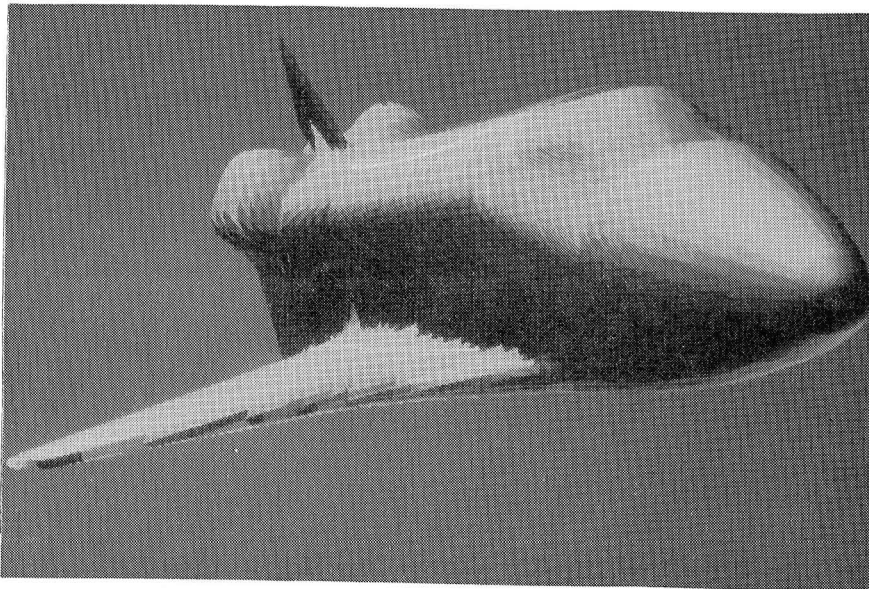


Fig. 4 Oil flow pattern,  $M_\infty = 7.9$ ,  $\alpha = 25^\circ$  (Ref. 2)

### Example 2

The second example is a solution by Rizk, Steger, and Chaussee (Ref. 4) for the thin-layer Navier-Stokes equations with a perfect gas free stream. The flow field was subdivided into four regions, as shown in Fig. 5, to accommodate different grids and numerical methods and to make effective use of the available computer storage. Region I was solved first, and results at a downstream plane, where the flow was supersonic, was used as in-

put for Region II calculations. This procedure was repeated for Regions III and IV. Time-dependent procedures were used in all four regions, although a space-marching method could have been implemented in Region III to conserve computer time.

Results are presented at the aft fuselage station,  $x/L = 0.91$ , in Fig. 6 for  $M_\infty = 1.4$ ,  $\alpha = 0^\circ$ , and turbulent flow, using the Baldwin-Lomax model. Details of the computational grid near the body are shown in Fig. 6a, including the wing, orbital maneuvering system pod, and vertical tail. Isobars are shown in Fig. 6b.

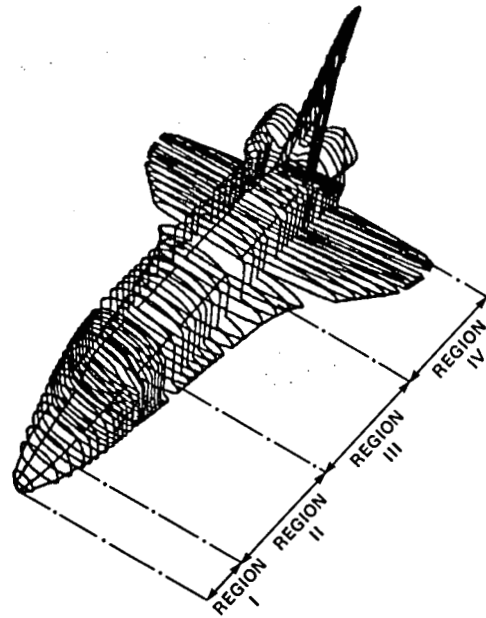


Fig. 5 Computational regions (Ref. 4)

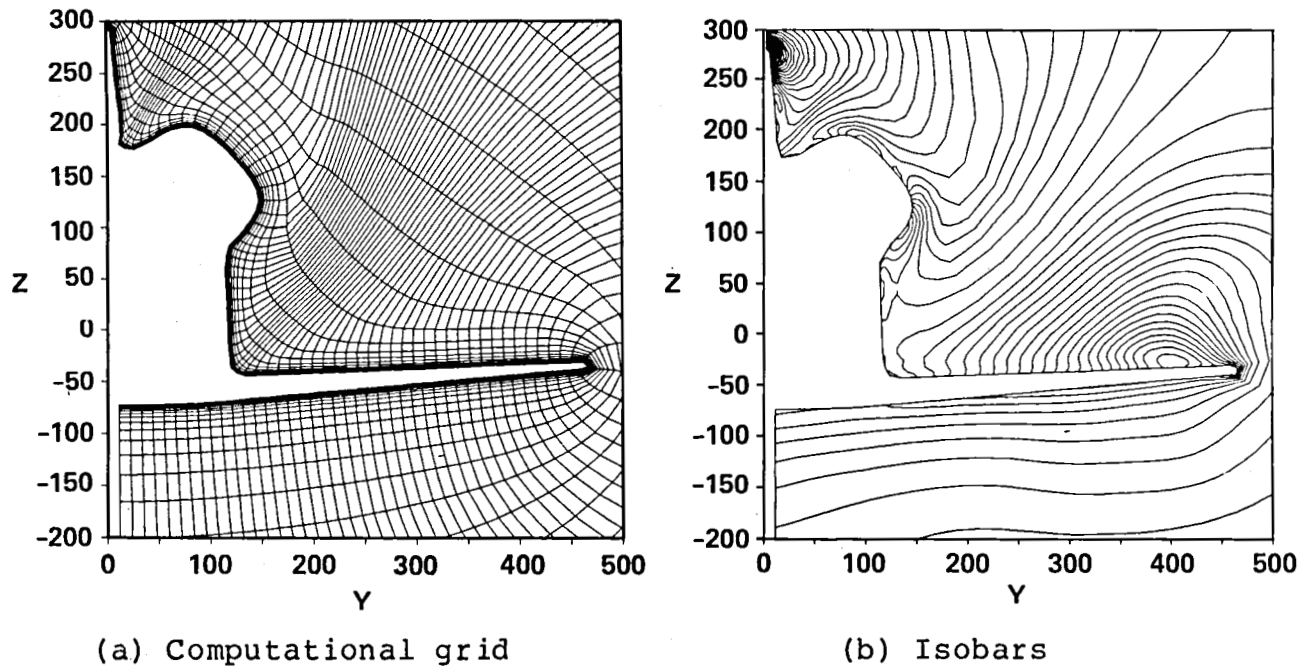


Fig. 6 Perfect gas solution,  $M_\infty = 1.4$ ,  $\alpha = 0^\circ$ ,  $x/L = 0.91$  (Ref. 4)

Example 3

The third example is a solution by Prabhu and Tannehill

(Ref. 5), which incorporates real-gas effects in a parabolized Navier-Stokes code. The thermodynamic properties were obtained from curve fits to tables that are applicable for equilibrium air at high temperatures, including the effects of dissociation and ionization. A modified orbiter geometry, deleting the canopy, vertical tail, and orbital maneuvering system pods, was used for the calculations.

The parabolized Navier-Stokes equations were solved, beginning at  $x/L = 0.015$ , with initial conditions obtained from a blunt-body code for the nose region. The flow field properties were marched downstream until terminated at  $x/L = 0.40$  by numerical difficulties attributed to the grid generation method. Mach number contours at  $x/L = 0.40$  are shown in Fig. 7 for laminar flow at  $M_\infty = 21$ ,  $\alpha = 40^\circ$ , and an altitude of 71.3 km.

#### Example 4

The last example is a solution by Balakrishnan (Ref. 6), which also incorporates real-gas effects in a parabolized Navier-Stokes code. In this case, however, the species concentrations and thermodynamic properties were calculated at each grid point

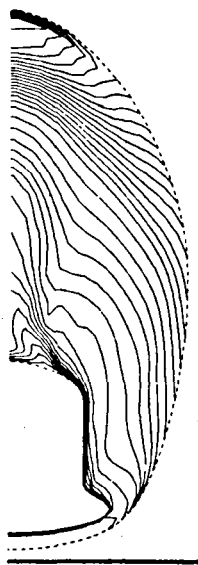


Fig. 7 Real gas solution, Mach contours,  $M_\infty = 21$ ,  $\alpha = 40^\circ$ , altitude = 71.3 km,  $x/L = 0.4$  (Ref. 5)

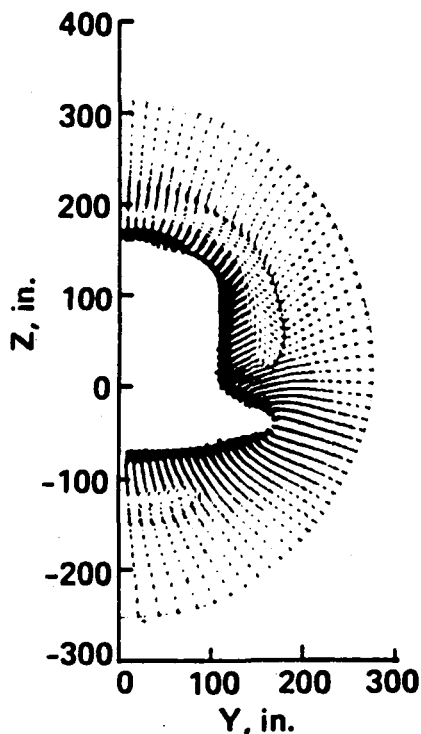


Fig. 8 Real gas solution, cross-flow velocity vectors,  $M_\infty = 13$ ,  $\alpha = 0^\circ$ , altitude = 55.8 km,  $x/L = 0.53$  (Ref. 6)



using formulations obtained from the kinetic theory of gases. Air was assumed to be composed of seven species in thermodynamic equilibrium, including oxygen, nitrogen, and nitric oxide molecules; oxygen and nitrogen atoms; nitric oxide ions; and electrons. Although requiring more computer time, this approach provides species mole fractions necessary for calculating radiative heat transfer and is readily extendible to nonequilibrium flow calculations. The simplified geometry of the third example was also used for these calculations.

Initial conditions at the cross section,  $x/L = 0.026$ , which were obtained from a blunt body solution, were marched downstream to  $x/L = 0.61$ . Cross-flow velocity vectors at the cross section,  $x/L = 0.53$ , are shown in Fig. 8 for laminar flow at  $M_\infty = 13$ ,  $\alpha = 0^\circ$ , and an altitude of 55.8 km. Flow reversal is indicated at the wing-body juncture.

#### CONCLUDING REMARKS

Computer simulations can now provide detailed information about the viscous flow around the space shuttle orbiter for a wide range of free-stream Mach and Reynolds numbers and gas properties. Computer codes validated by wind tunnel tests can be applied at flight conditions which cannot be reproduced in test facilities. The aerodynamic design of the Space Shuttle orbiter was fixed 10 years ago, but computer simulations are useful today, for example, for studies of a crew escape system during the launch phase. In addition, the computer codes can be used for preliminary design studies of advanced aerospace vehicles.

#### REFERENCES

1. M. Inouye, "Computer Simulation of Hypersonic Flow over the Space Shuttle Orbiter," Proc. of 12th ISTS, pp. 103-108, Tokyo, 1977.
2. D.S. Chaussee, Y.M. Rizk, P.G. Buning, "Viscous Computation of a Space Shuttle Flow Field," 9th Intern. Conf. on Numerical Methods in Fluid Dynamics, Saclay, France, June 25-29, 1984.
3. B.S. Baldwin, H. Lomax, "Thin Layer Approximation and Algebraic Model for Separated Turbulent Flows," AIAA 16th Aerospace Sciences Meeting Paper No. 78-257, Huntsville, AL, Jan. 16-18, 1978.
4. Y.M. Rizk, J.L. Steger, D.S. Chaussee, "Use of a Hyperbolic Grid Generation Scheme in Simulating Supersonic Viscous Flow about Three-Dimensional Winged Configurations," in Numerical Methods in Fluid Mechanics II, Proc. of Intern.

Symp. on Computational Fluid Dynamics - Tokyo, pp. 392-403, Tokyo, 1985.

5. D.K. Prabhu, J.C. Tannehill, "Numerical Solution of Space Shuttle Orbiter Flowfield Including Real-Gas Effects," *Journal of Spacecraft and Rockets*, Vol.23, No.3, May-June 1986, pp. 264-272.
6. A. Balakrishnan, "Computation of a Viscous Real Gas Flowfield for the Space Shuttle Orbiter," *AIAA 19th Thermophysics Conf. Paper No. 84-1748*, Snowmass, CO, June 25-28, 1984.



# Report Documentation Page

1. Report No. <b>NASA TM-100990</b>		2. Government Accession No.		3. Recipient's Catalog No.	
4. Title and Subtitle <b>A Decade of Computer Simulations for Space Shuttle Aerodynamics</b>				5. Report Date <b>May 1988</b>	
				6. Performing Organization Code	
7. Author(s) <b>Mamoru Inouye</b>				8. Performing Organization Report No. <b>A-88150</b>	
				10. Work Unit No. <b>505-60-01</b>	
9. Performing Organization Name and Address <b>Ames Research Center Moffett Field, CA 94035</b>				11. Contract or Grant No.	
				13. Type of Report and Period Covered <b>Technical Memorandum</b>	
12. Sponsoring Agency Name and Address <b>National Aeronautics and Space Administration Washington, DC 20546-0001</b>				14. Sponsoring Agency Code	
				15. Supplementary Notes  <b>Point of Contact: Mamoru Inouye, Ames Research Center, MS 202-1 Moffett Field, CA 94035 (415) 694-5126 or FTS 464-5126</b>	
16. Abstract  Ten years ago, computer simulations of the flow field around the Space Shuttle orbiter were limited to inviscid calculations for the windward side of the forebody and viscous calculations for selected two-dimensional problems. Advances in computer hardware and numerical methods during the past 10 years have made it possible to calculate viscous flow over the complete orbiter configuration at angle of attack. The equations solved are the Reynolds-averaged, Navier-Stokes equations, simplified by either the thin-layer or parabolized approximation. An algebraic eddy viscosity model is used for turbulent flow. The free stream is assumed to be a perfect gas for wind tunnel conditions and a real gas in thermodynamic equilibrium for flight conditions. Four examples of recent computer simulations will be presented. Flow field results include oil flow patterns on the surface and Mach number contours, isobars, and cross-flow velocity vectors in the shock layer.					
17. Key Words (Suggested by Author(s)) <b>Space Shuttle Aerodynamics Computational fluid dynamics</b>			18. Distribution Statement <b>Unclassified-Unlimited</b>  <b>Subject Category - 02</b>		
19. Security Classif. (of this report) <b>Unclassified</b>		20. Security Classif. (of this page) <b>Unclassified</b>		21. No. of pages <b>8</b>	22. Price <b>A02</b>